

Research Article

Int J Energy Studies 2023; 8(4): 849-858

DOI: 10.58559/ijes.1372882

Received : 08 Oct 2023

Revised : 16 Oct 2023

Accepted : 16 Oct 2023

## Photovoltaic properties of Cu(In,Ga)(Se,Te)<sub>2</sub> thin film solar cells with different tellurium amounts and a copper-poor stoichiometry

Semih Ağca<sup>a\*</sup>, Güven Çankaya<sup>b</sup>

<sup>a</sup>Department of Metallurgical and Materials Engineering, Faculty of Engineering and Natural Sciences, Ankara Yıldırım Beyazıt University, Ankara, 06010, Türkiye, ORCID: 0000-0002-4834-5337

<sup>b</sup>Department of Metallurgical and Materials Engineering, Faculty of Engineering and Natural Sciences, Ankara Yıldırım Beyazıt University, Ankara, 06010, Türkiye, ORCID: 0000-0003-2932-1695

(\*Corresponding Author: semihagca@aybu.edu.tr)

### Highlights

- Cu(In,Ga)(Se,Te)<sub>2</sub> thin film solar cells were produced by three-stage co-evaporation process
- The addition of tellurium decreased the surface roughness and increased the crystal quality of the absorber
- Optimum photovoltaic properties and the best efficiency were obtained with sample having 1.1 tellurium atomic percentage.
- The efficiency of the solar cell was successfully increased from 9.7% to 10.6% by addition of tellurium.

**You can cite this article as:** Ağca S, Çankaya G. Photovoltaic properties of Cu(In,Ga)(Se,Te)<sub>2</sub> thin film solar cells with different tellurium amounts and a copper-poor stoichiometry. Int J Energy Studies 2023; 8(4): 849-858.

### ABSTRACT

In this study, the impact of tellurium addition on the microstructure of the copper indium gallium selenide absorber layer with a copper-poor stoichiometry and the photovoltaic properties of SLG/Mo/CIGS/CdS/ZnO/ITO/Ni-Al-Ni solar cells was investigated. Absorber layer, CdS buffer, ZnO and ITO layers, and the Ni-Al-Ni front contact were produced using three-stage co-evaporation, chemical bath deposition, RF magnetron sputtering, and e-beam evaporation techniques, respectively. The thickness and the composition of the absorber layer were controlled in situ. NaF post deposition treatment were applied to the absorber layer. The addition of tellurium improved the crystal quality by increasing the average grain size and decreased the surface roughness. Decreasing surface roughness increased reflection and thus decreased the amount of sunlight absorbed, which in turn reduced current collection. Open-circuit voltage was effected by impurity level and the grain boundry recombination. While moderate tellurium addition reduced grain boundary recombination, excessive tellurium addition created stress, caused crack formation, and increased recombination by reducing crystal quality. The optimum tellurium amount in the copper-poor CIGS structure was found to be 1.1 atomic percent. The control of the microstructure of the absorber and the efficiency improvement of the solar cell were achieved successfully.

**Keywords:** Thin film, Solar cell, Tellurium, Copper-poor stoichiometry

## 1. INTRODUCTION

Increasing energy needs and high amounts of carbon emissions, which have become a serious problem, have led researchers to turn to alternative green, renewable, and sustainable energy sources [1]. Solar energy stands out among other renewable energy sources with its wide potential. Although there are many energy production methods in which solar energy is in the background, there are photovoltaic systems that can produce electrical energy directly from sunlight. They can be classified as silicon, gallium arsenide (GaAs), copper indium gallium selenide (CIGS), copper zinc tin sulfide (CZTS), perovskite, and organic solar cells. Among these, CIGS solar cells are very advantageous due to their features such as adjustable bandgap, low material usage, stability, high efficiency, and high absorption coefficient [2-10]. Moreover, due to its high radiation tolerance, it can be used in both terrestrial and space applications [11].

CIGS solar cells are generally produced on soda lime glass (SLG) substrates. However, metal or polymer flexible substrates can also be used [12,13]. Molybdenum is generally preferred as the back contact material. The layers after the back contact are p-type CIGS absorber, n-type buffer, window, and transparent conductive oxide (TCO) layers, respectively. After the deposition of the front contact, the circuit is completed.

Among the layers of CIGS solar cells, the absorber layer is the most researched and the most important one. It is very difficult to control the thickness, composition, and microstructure of the absorber layer, and these parameters directly affect the efficiency of the solar cell. In this study, the thickness and the composition of the absorber layer were controlled via a real-time in situ system and an attempt was made to achieve microstructure control by adding tellurium. Furthermore, the effect of tellurium on the microstructure of the absorber and the parameters of SLG/Mo/CIGS/CdS/ZnO/ITO/Ni-Al-Ni solar cells was investigated.

## 2. EXPERIMENTAL DETAILS

The absorber layer was deposited on a molybdenum-coated SLG substrate by a three-stage co-evaporation method. The pressure of the vacuum chamber and the substrate temperature were  $2 \times 10^{-7}$  mBar and 620 °C, respectively. 2  $\mu$ m thickness and the desired compositions were obtained by laser light scattering (LLS) system in situ. NaF post-deposition treatment (PDT) was applied to improve the photovoltaic performance of the solar cells. The Cu/(Ga+In) (CGI) and Ga/(Ga+In) (GGI) ratios of the absorber layer were set to 0.8 and 0.3, respectively. Different absorber layer

compositions were set by adding 0, 0.5, 0.8, 1.1, and 1.4 atomic percentages of tellurium. Therefore, the samples were named Te0, Te0.5, Te0.8, Te1.1, and Te1.4.

The CdS buffer layer was deposited by a chemical bath deposition technique with 50 nm thickness. Zinc oxide (ZnO) window and indium tin oxide (ITO) TCO layers were deposited by RF magnetron sputtering with 100 nm and 200 nm thicknesses, respectively. Ni-Al-Ni front contacts were deposited by e-beam evaporation. The nickel layers had a thickness of 30 nm, while the thickness of the aluminum layer was 2  $\mu\text{m}$ . After the mechanical scribing, the area of the solar cells was approximately 0.5  $\text{cm}^2$ .

The top-view scanning electron microscope (SEM) microstructure photographs of absorber layers were taken by ZEISS Supra 40VP SEM after the PDT process. The chemical composition of the absorber layers was determined by Bruker EDS which was attached to the SEM. The photovoltaic parameters were obtained by using external quantum efficiency (EQE) and current density-voltage (J-V) measurement techniques with a four-point measurement setup and a xenon lamp equipped with a monochromator under AM1.5G standard test conditions at room temperature.

### 3. RESULTS AND DISCUSSION

The chemical composition of the absorbers which was obtained by EDS is shown in Table 1.

**Table 1.** The chemical composition of the absorber layers

Sample	Cu at. %	In at. %	Ga at. %	Se at. %	Te at. %
Te0	21.5	18.7	6.9	52.9	0
Te0.5	21.3	18.9	6.7	52.6	0.5
Te0.8	20.9	17.7	7.7	52.9	0.8
Te1.1	20.8	17.4	7.9	52.8	1.1
Te1.4	20.2	18.3	7.8	52.3	1.4

It can be calculated from Table 1 that, the GGI ratio of the absorbers was found to be around 0.3 which is the desired ratio to fabricate highly efficient solar cells [14]. On the other hand, the CGI ratio of the absorbers was found to be around 0.8 which corresponds to a copper-poor stoichiometry when compared with the solar cell studies in the literature having an absorber with a CGI of 0.9 [15]. The top-view SEM microstructure photographs of the absorber layers are shown in Figure 1.

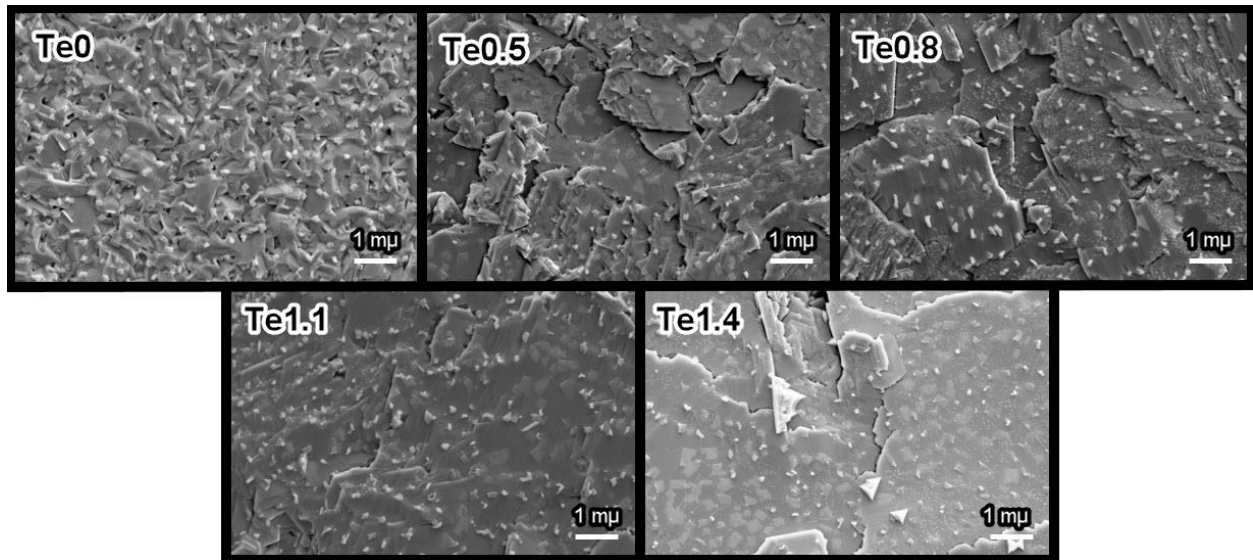


**Figure 1.** The top-view SEM microstructure photographs of the absorber layers

As can be seen in Figure 1, the addition of tellurium decreased the surface roughness and increased the average grain size. The increase in average grain size with tellurium addition is in good agreement with the literature [16,17]. On the other hand, it was observed that the surface roughness increased with the addition of tellurium in the CIGS compound containing high gallium in another study [18]. The decrease in surface roughness with increasing tellurium amount may be due to the fact that we used lower CGI and GGI values than the literature. The small white particles represent the residual NaF PDT on the surface. The addition of tellurium improved the crystal quality by enlarging the CIGS structure in the horizontal direction. However, it was observed that crack formation began in the microstructure when the tellurium amount reached 1.4 atomic percent. When the added tellurium replaced selenium, the lattice may have been distorted and stress may have been produced due to tellurium having a larger atomic radius than selenium [16]. As the amount of tellurium increased further, the amount of stress may have increased and eventually caused crack propagation due to atomic radius difference.

After the microstructure photographs were taken, other layers were deposited on the absorber layer and a solar cell with an SLG/Mo/CIGS/CdS/ZnO/ITO/Ni-Al-Ni structure was produced. The reason why nickel is deposited under and on the aluminum in the front contact is to prevent the aluminum from diffusing into the structure and also from oxidizing and reducing its conductivity. After mechanical scribing, four solar cells with an area of approximately  $0.5 \text{ cm}^2$  were formed from each composition. Photovoltaic characterization results of only the best solar cells from each composition are presented. EQE measurement results of the best solar cells are shown in Figure 2.

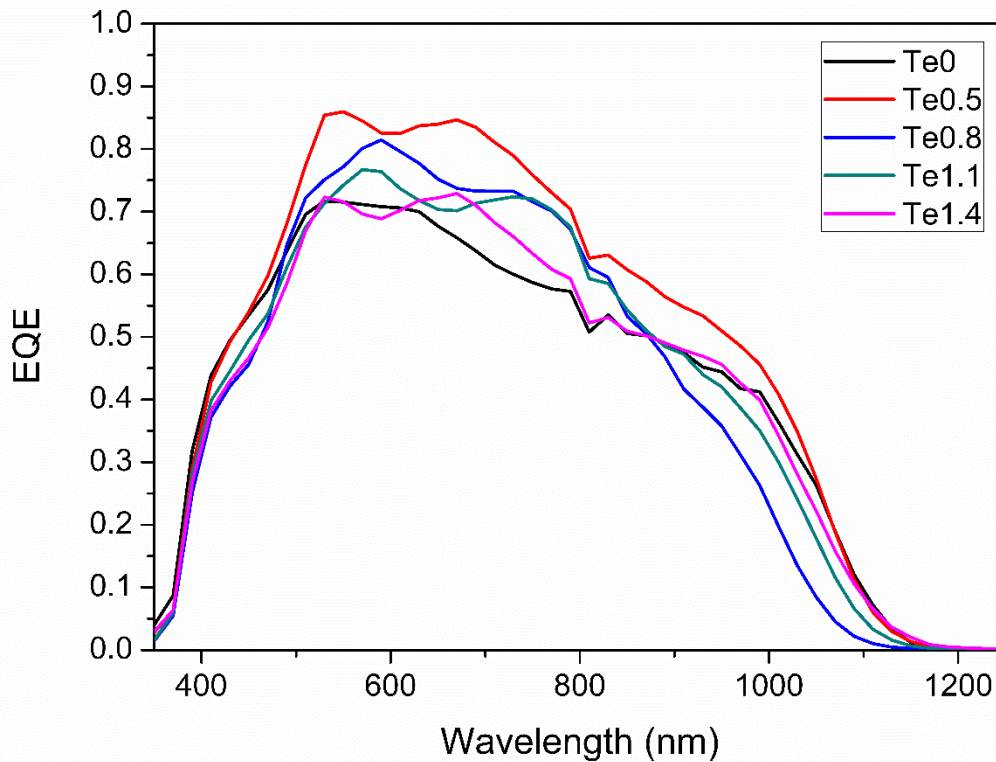


**Figure 2.** EQE measurement results of the best solar cells

As can be seen in Figure 2, the current collection varied with different regimes at different tellurium amounts. When comparing Te0 and Te0.5 solar cells, it was seen that the addition of a small amount of tellurium increased the current collection at all wavelengths. On the other hand, as the amount of tellurium increased further, different decreases in the current collection were detected at different wavelengths. While it decreased less between 400 and 850 nm wavelength, it decreased more when the wavelength was larger than 850 nm.

It is predicted that the effect of tellurium addition on current collection occurs differently on the surface and inside the absorber. As the amount of tellurium increased, the optical properties inside the absorber changed with the increase in crystal quality and average grain size, increasing the current collection [19]. The basic mechanism here may be that, depending on the microstructure and grain size, sunlight is refracted more within the absorber, thus increasing the light path and increasing the probability of collection [20]. On the other hand, the situation is different on the surface. Decreasing surface roughness increased reflection and thus decreased the amount of sunlight absorbed, which in turn reduced current collection [21]. J-V measurement results of the best solar cells are shown in Figure 3.

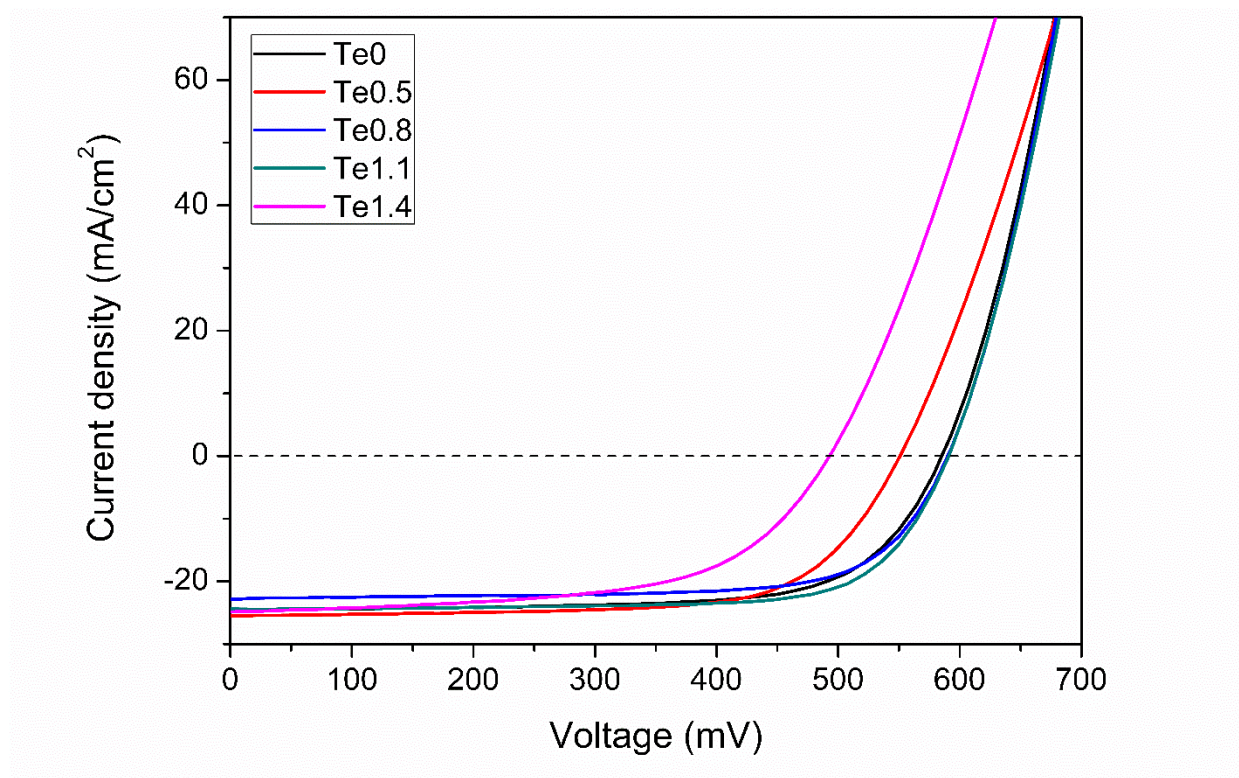


**Figure 3.** J-V measurement results of the best solar cells

It can be seen in Figure 3 that, the addition of tellurium affected open-circuit voltage ( $V_{oc}$ ) and short-circuit current density ( $J_{sc}$ ) in different manners. Moreover, it has been observed that the fill factor (FF) varies differently with different tellurium amounts. Photovoltaic parameters and power conversion efficiencies (PCE) of the best solar cells are shown in Table 2.

**Table 2.** Photovoltaic parameters of the best solar cells

Sample	$V_{oc}$ (mV)	$J_{sc}$ (mA/cm <sup>2</sup> )	FF (%)	PCE (%)
Te0	584	24.9	66.4	9.7
Te0.5	551	25.5	68.4	9.6
Te0.8	571	23.5	70.9	9.5
Te1.1	591	24.4	73.2	10.6
Te1.4	430	24.8	59.1	7.2

Changes in  $J_{sc}$  are mainly related to optical properties and were explained together with the EQE results.  $V_{oc}$  value first decreased with the addition of tellurium from 584 mV to 551 mV, and then increased with further increasing tellurium amount up to 591 mV. When the amount of tellurium reached 1.4 atomic percent, the  $V_{oc}$  decreased significantly to 430 mV. First of all,  $V_{oc}$  decreased

because the tellurium added to the CIGS structure acted as impurity and caused recombination [22]. Although there is grain growth at low amounts of tellurium addition, the impurity effect is more dominant than the crystal quality effect. When the amount of tellurium was further increased, the grain size increased significantly and reduced the amount of grain boundaries, which are recombination centers. Thus, Voc increased as grain boundary recombination decreased [23]. When the atomic percentage of tellurium reached 1.4, cracks appeared on the surface due to the stress caused by excessive distortion of the crystal lattice originating from the difference between the atomic radius of Te and Se [16]. Since these cracks and defects produced by excessive distortion both reduce crystal quality and increase recombination, Voc decreased drastically.

The addition of tellurium increased the FF by preventing the formation of disorder at the absorber/CdS interface by increasing the absorber crystal quality [24,25]. In the solar cell where the atomic percentage of tellurium is 1.4, the FF decreased significantly due to the deterioration of the absorber/CdS interface [26]. Consequently, the solar cell with an atomic percentage of tellurium of 1.1 has the highest PCE value with the highest Voc and FF and medium Jsc values.

#### 4. CONCLUSION

The effect of tellurium on the microstructure of the absorber and the photovoltaic parameters of SLG/Mo/CIGS/CdS/ZnO/ITO/Ni-Al-Ni solar cells was investigated. The addition of tellurium decreased the surface roughness and increased the crystal quality of the absorber by enlarging the CIGS structure in the horizontal direction. However, the addition of excessive amounts of tellurium produced stress and caused crack formation.

The effect of tellurium on the current collection was different for the surface and the bulk. While the main mechanism on the surface was more reflection due to less roughness, it was the light trapping resulting longer light path and increased collection probability. The Voc was affected by two mechanisms: impurity and grain boundary recombination. The increase in tellurium increased the FF until cracks formed due to excess tellurium and disrupted the absorber/CdS interface. As a conclusion, although there is always a compromise in solar cell properties, optimized values and the best PCE were obtained in the solar cell with 1.1 tellurium atomic percentage. By adding tellurium to the CIGS solar cell, the microstructure was successfully controlled and the efficiency was increased by improving the photovoltaic parameters. The power conversion efficiency of the solar cell was successfully increased from 9.7% to 10.6% by the addition of tellurium.

## ACKNOWLEDGMENT

This study was supported by TÜBİTAK 2214-A and TÜBİTAK 2211-C Scholarship Programmes. We would like to thank to PV Group of Prof. Dr. Roland Scheer in the Physics Institute of Martin-Luther University Halle-Wittenberg for their support with the laboratory infrastructure.

## DECLARATION OF ETHICAL STANDARDS

The authors of the paper submitted declare that nothing which is necessary for achieving the paper requires ethical committee and/or legal-special permissions.

## CONTRIBUTION OF THE AUTHORS

**Semih Ağca:** Performing the experiments and analyzing the results, writing the manuscript.

**Güven Çankaya:** Bringing the idea, supervising the study, final check of the manuscript.

## CONFLICT OF INTEREST

There is no conflict of interest in this study.

## REFERENCES

- [1] Bulbul S, Ertugrul G, Arli F. Investigation of usage potentials of global energy systems. *International Advanced Researches and Engineering Journal* 2018; 2: 58-67.
- [2] Lee TD, Ebong AU. A review of thin film solar cell technologies and challenges. *Renewable and Sustainable Energy Reviews* 2017; 70: 1286-1297.
- [3] Jäger-Waldau A. Status and perspectives of thin film photovoltaics - Thin film solar cells: Current status and future trends. Nova Science Publishers Inc, New York, US, 2010.
- [4] Fiat S, Polat I, Bacaksiz E, Çankaya G, Koralli P, Manolakos DE, Kompitsas M. Optical and structural properties of nanostructured  $\text{CuIn}_{0.7}\text{Ga}_{0.3}(\text{Se}_{1-x}\text{Te}_x)_2$  chalcopyrite thin films—Effect of stoichiometry and annealing. *Journal of Nanoscience and Nanotechnology* 2014; 14: 5002-5010.
- [5] Poortmans J, Arkhipov V. Thin film solar cells: Fabrication, characterization, and applications. John Wiley & Sons, West Sussex, England, 2006.
- [6] Varol SF, Bacaksiz E, Koralli P, Kompitsas M, Çankaya G. A novel nanostructured  $\text{CuIn}_{0.7}\text{Ga}_{0.3}(\text{Se}_{0.4}\text{Te}_{0.6})_2/\text{SLG}$  multinary compounds thin films: For photovoltaic applications. *Materials Letters* 2015; 142: 273-276.

- [7] Fiat S, Polat İ, Bacaksiz E, Kompitsas M, Çankaya G. The influence of annealing temperature and tellurium (Te) on electrical and dielectrical properties of Al/p-CIGSeTe/Mo Schottky diodes. *Current Applied Physics* 2013; 13: 1112-1118.
- [8] Karatay A, Küçüköz B, Çankaya G, Ates A, Elmali A. The effect of Se/Te ratio on transient absorption behavior and nonlinear absorption properties of  $\text{CuIn}_{0.7}\text{Ga}_{0.3}(\text{Se}_{1-x}\text{Te}_x)_2$  ( $0 \leq x \leq 1$ ) amorphous semiconductor thin films. *Optical Materials* 2017; 73: 20-24.
- [9] Fiat S, Bacaksiz E, Kompitsas M, Çankaya G. Temperature and tellurium (Te) dependence of electrical characterization and surface properties for a chalcopyrite structured Schottky barrier diode. *Journal of Alloys and Compounds* 2014; 585: 178-184.
- [10] Varol SF, Bacaksız E, Çankaya G, Kompitsas M. Optical, structural, and morphological characterization of  $\text{CuIn}_{0.7}\text{Ga}_{0.3}(\text{Se}_{0.6}\text{Te}_{0.4})_2$  thin films under different annealing temperatures. *Celal Bayar University Journal of Science* 2013; 9: 9-16.
- [11] Minoura S, Kodera K, Maekawa T, Miyazaki K, Niki S, Fujiwara H. Dielectric function of Cu(In, Ga)Se<sub>2</sub>-based polycrystalline materials. *Journal of Applied Physics* 2013; 113: 063505.
- [12] Conibeer GJ, Willoughby A. *Solar cell materials: Developing technologies*. John Wiley and Sons Ltd, England, 2014.
- [13] Başol BM, Kapur VK, Leidholm CR, Halani A, Gledhill K. Flexible and lightweight copper indium diselenide solar cells on polyimide substrates. *Solar Energy Materials and Solar Cells* 1996; 43: 93-98.
- [14] Wei SH, Zhang SB, Zunger A. Effects of Ga addition to CuInSe<sub>2</sub> on its electronic, structural, and defect properties. *Applied Physics Letters* 1998; 72: 3199-3201.
- [15] Naghavi N, Mollica F, Goffard J, Posada J, Duchatelet A, Jubault M, Donsanti F, Cattoni A, Collin S, Grand PP, Greffet JJ, Lincot D. Ultrathin Cu(In,Ga)Se<sub>2</sub> based solar cells. *Thin Solid Films* 2017; 633: 55-60.
- [16] Atasoy Y, Başol B, Olğar M, Tomakin M, Bacaksız E. Cu(In,Ga)(Se,Te)<sub>2</sub> films formed on metal foil substrates by a two-stage process employing electrodeposition and evaporation. *Thin Solid Films* 2018; 649: 30-37.
- [17] Atasoy Y, Başol B, Polat İ, Tomakin M, Parlak M, Bacaksız E. Cu(In,Ga)(Se,Te)<sub>2</sub> pentenary thin films formed by reaction of precursor layers. *Thin Solid Films* 2015; 592: 189-194.
- [18] Ağca S, Çankaya G, Sonmezoglu S. Impact of tellurium as an anion dopant on the photovoltaic performance of wide-bandgap Cu(In,Ga)Se<sub>2</sub> thin-film solar cells with rubidium fluoride post-deposition treatment. *Frontiers in Energy Research* 2023; 11: 1215712.

- [19] Singh R, Parashar M, Sandhu S, Yoo K, Lee JJ. The effects of crystal structure on the photovoltaic performance of perovskite solar cells under ambient indoor illumination. *Solar Energy* 2021; 220: 43-50.
- [20] Saive R. Light trapping in thin silicon solar cells: A review on fundamentals and Technologies. *Progress in Photovoltaics: Research and Applications* 2021; 29:1125-1137.
- [21] Scholtz L, Ladanyi, L, Mullerova J. Influence of surface roughness on optical characteristics of multilayer solar cells. *Advances in Electrical and Electronic Engineering* 2015; 12: 631-638.
- [22] Karki S, Paul P, Rajan G, Belfore B, Poudel D, Rockett A, Danilov E, Castellano F, Arehart A, Marsillac S. Analysis of recombination mechanisms in RbF treated CIGS solar cells. *IEEE Journal of Photovoltaics* 2018; 9: 313-318.
- [23] Gloeckler M, Sites JR, Metzger WK. Grain-boundary recombination in Cu(In,Ga)Se<sub>2</sub> solar cells. *Journal of Applied Physics* 2005; 98: 113704.
- [24] Xing G, Mathews N, Sun S, Lim SS, Lam YM, Gratzel M, Mhaisalkar S, Sum TC. Long-range balanced electron-and hole-transport lengths in organic-inorganic CH<sub>3</sub>NH<sub>3</sub>PbI<sub>3</sub>. *Science* 2013; 342: 344-347.
- [25] Yin WJ, Chen H, Shi T, Wei SH, Yan Y. Origin of high electronic quality in structurally disordered CH<sub>3</sub>NH<sub>3</sub>PbI<sub>3</sub> and the passivation effect of Cl and O at grain boundaries. *Advanced Electronic Materials* 2015; 1: 1500044.
- [26] Guirdjebaye N, Ngoupo AT, Ouedraogo S, Tcheum GLM, Ndjaka JMB. Numerical analysis of CdS-CIGS interface configuration on the performances of Cu(In,Ga)Se<sub>2</sub> solar cells. *Chinese Journal of Physics* 2020; 67: 230-237.